Research Square

Preprints are preliminary reports that have not undergone peer review.
They should not be considered conclusive, used to inform clinical practice,
or referenced by the media as validated information.

Concurrent low-dose-rate gamma irradiation and inorganic arsenite: genotoxicity and transcriptional responses in liver and testis in CBA and C57BL/6 mice

Dag M Eide

Dag.Marcus.Eide@fhi.no

Norwegian Institute of Public Health

Anne Graupner

Federal Office for Radiation Protection

Birgitte Lindeman

Norwegian Institute of Public Health

Hildegunn Dahl

Norwegian Radiation and Nuclear Safety Authority

Dag A Brede

Norwegian University of Life Sciences

Nur Duale

Norwegian Institute of Public Health

Ann Karin Olsen

NILU

Research Article

Keywords: inorganic arsenic, low-dose-rate gamma radiation, co-exposure, genotoxicity, comet assay, RNA-seq, liver, testis, oxidative DNA damage

Posted Date: July 31st, 2026

DOI: https://doi.org/10.21203/rs.3.rs-10353671/v1

License: This work is licensed under a Creative Commons Attribution 4.0 International License.
Read Full License

Additional Declarations: No competing interests reported.

Version of Record: A version of this preprint was published at Archives of Toxicology on November 3rd, 2026. See the published version at https://doi.org/10.1007/s00204-026-04626-2.

Concurrent low-dose-rate gamma irradiation and inorganic arsenite: genotoxicity and transcriptional responses in liver and testis in CBA and C57BL/6 mice

Dag M Eide[1,6]*, Anne Graupner[2,6], Birgitte Lindeman[1,6], Hildegunn Dahl[4,6], Dag A Brede[5,6], Nur Duale [1,6], Ann Karin Olsen[3,6]

[1]Department of Chemical Toxicology, Norwegian Institute of Public Health, Oslo 0403, Norway
[2]Bundesamt für Strahlenschutz (BfS) 10318 Berlin, Germany
[3] Department for Environmental Chemistry and Health Effects, NILU, Kjeller, NO-2007, Norway
[4]Department of Research, Norwegian Radiation Protection Authority, Østerås 1361, Norway
[5]Department of Environmental Sciences, Norwegian University of Life Sciences, Ås 1432, Norway
[6]Centre for Environmental Radioactivity (CoE CERAD), Ås 1432, Norway

*Corresponding author:

Dag Eide, Department of Chemical Toxicology, Norwegian Institute of Public Health, Oslo 0403, Norway

Abstract

Humans in arsenic-endemic and radiologically exposed settings may be co-exposed to inorganic arsenic and ionizing radiation, yet the combined effects of chronic low-dose-rate irradiation and environmentally relevant arsenic are poorly defined. In a single factorial experiment, male CBA and C57BL/6N mice were exposed to sodium arsenite in drinking water (0, 0.3 or 3 mg/L) and chronic γ irradiation (2.5 mGy/h, total 3 Gy), alone and combined. We measured blood genotoxicity (comet and micronucleus assays), characterised 21 circulating miRNAs, and sequenced liver and testis transcriptomes, analysing all endpoints in a factorial model (arsenite × irradiation × strain).

Arsenite exposure was accompanied by an increase in oxidative DNA lesions in white blood cells along a slight reduction in single strand breaks. Micronucleus frequency in reticulocytes and erythrocytes was not affected by arsenite. Arsenite was identified as an oxidative rather than a chromosomal genotoxicant. The liver and testis transcriptomes shared a common DNA-repair and oxidative-stress response that diverged between the organs. Irradiation was the dominant stressor while the concurrent arsenite exposure was mainly non-additive or counteracting, but also additive effects were observed. Only two miRNAs responded to arsenite. Baseline strain differences were large but additive, with negligible strain×treatment interaction.

Our study contributes new data, experimental design and analysis methods about the genotoxic and transcriptional landscape of multiple stressor exposures.

Keywords: inorganic arsenic; low-dose-rate gamma radiation; co-exposure; genotoxicity; comet assay; RNA-seq; liver; testis; oxidative DNA damage

1 Introduction

Humans are exposed to ionising radiation through occupational and clinical settings, accidents and contaminated food. The arsenic exposure is mainly through contaminated drinking water and food, affecting millions worldwide. High-dose radiation causes DNA double-strand breaks, clastogenic and oxidative DNA lesions and raises the risk of cancer and of cardiovascular and metabolic disease. The effects of chronic low-dose-rate exposure (≤5 mGy/h) are far less clear. Chronic inorganic arsenic exposure is likewise associated with skin lesions, hepatotoxicity, cardiovascular disease and diabetes (WHO, 2001). Arsenic is recognised as a weak mutagen and human co-carcinogen, acting largely through reactive oxygen species and impaired DNA repair rather than direct mutagenesis (IARC, 2012).

People are co-exposed to radiation and arsenic in settings such as uranium mining and radiological exposure in arsenic-endemic regions (Corcho Alvarado et al., 2014; Skipperud et al., 2013). High arsenic concentrations potentiate radiotherapy, attributed to increased ROS and reduced DNA-repair capacity (Zhang et al., 2025). Whether and how low-dose-rate radiation and environmentally relevant arsenic doses interact is largely unknown: existing combined-exposure studies have focused mainly on skin and keratinocytes (Berglund et al., 2009), and no *in vivo* study has examined chronic low-dose-rate γ-irradiation combined with low-dose arsenite across multiple tissues and endpoints.

We therefore conducted an experiment in male mice combining genotoxicity assays, miRNA profiling and RNA sequencing of liver and testis after chronic low-dose-rate γ-irradiation and arsenite in drinking water. The factorial design allows the arsenite effect, the irradiation effect and their interaction to be estimated jointly in two genetic backgrounds (CBA, B6N).

We wanted to test four hypotheses (H_A) against no effect (H_0): H_A1: arsenite is a mutagen at human relevant doses as detected by comet, micronucleus and transcriptomics. H_A2: co-exposure to arsenite and irradiation show additive genotoxic and transcriptional responses. H_A3: genotoxic and transcriptional responses to arsenate are strain-dependent shown as a strain×treatment interaction. Evidence for and against each hypothesis was quantified with Bayes inclusion factors (BF_{incl}) alongside frequentist significance testing.

2 Materials and methods

2.1 Animals, irradiation and arsenite exposure

We here report the arsenite-exposure part of the cohort described previously (Dahl et al., 2025). In brief, acclimated 8-week old male specific-pathogen-free CBA/CaOlaHsd (CBA) and C57BL/6NHsd (B6N) mice (Envigo, Horst, The Netherlands) were randomly assigned to groups receiving continuous γ-irradiation at 2.5 mGy/h for 1200 h (total 3 Gy, 53 days) or sham-irradiated in the same room behind lead shielding (<5 μGy/h); five mice in each cage mixing the strains with no aggressive behaviour observed. Husbandry and dosimetry were as reported (Dahl et al., 2025). The study complied with the European legislation for animal experiments and was approved ethically by the Norwegian Food Safety Authority (approval no. 8803).

New to this report is the arsenite exposure. Mice received sodium arsenite ($NaAsO_2$; Sigma Aldrich, 0.05 M solution, cat # S7400, purity >90%, EC #: 232-070-5) in the drinking water at 0.3 (Low As) or 3 mg/L (High As) from day 7 to day 53 of the irradiation period. A pilot study showed no detrimental health effects of these concentrations that are relevant for human exposures. The six exposure groups are presented in Table 1. The mice were anaesthetised one day after As-/γ-irradiation (zolazepam/tiletamine/xylazine/fentanyl) and exsanguinated by cardiac puncture. Liver, spleen, heart, testis and kidney were weighed, snap-frozen in liquid nitrogen and stored at −80 °C.

Table 1. Animal exposure groups

Treatment group	N	Arsenite mg/L in drinking water	γ-irradiation mGy/hrs (Gy)
Control	10	0	0
Low As	9	0.3	0
High As	8	3.0	0
Gamma (IR)	10	0	2.5 (3.2)
Low As + IR	9	0.3	2.5 (3.2)
High As + IR	10	3	2.5 (3.2)

2.2 Genotoxicity assays

DNA damage in blood leucocytes was measured by alkaline single-cell gel electrophoresis (comet assay) with and without formamidopyrimidine-DNA-glycosylase (FPG) as percentage tail intensity (% TI). The standard assay reports total single-strand breaks and alkali-labile sites (SSB/ALS) while FPG converts oxidised purines into additional strand breaks. The net oxidative DNA damage was calculated as FPG minus standard comet. Gels were scored semi-automatically (CometAssay IV, Perceptive Instruments). Blood micronucleus and comet assays were performed as described (Dahl et al., 2025; Graupner et al., 2016). Briefly, the percentage of reticulocytes (RET), micronucleated reticulocytes (MNRET) and normochromatic erythrocytes (MNNCE) were scored by flow cytometry (In Vivo Mouse MicroFlow^{PLUS} kit, Litron; BD LSR II) with 20,000 CD71-positive reticulocytes counted per sample. All procedures, including termination, were done in a random sequence and blinded to avoid experimenter bias.

2.3 Hepatic arsenic and zinc

Hepatic arsenic and zinc were determined by ICP-MS (Agilent8000) as previously described for Se-analysis (Graupner et al., 2015); reported as mg/kg (As) and g/kg (Zn). As-values below the limit of quantification (LOQ) were imputed as the reported uncertain value minus 0.01; values below the limit of detection (LOD) were set to LOD/2 (0.01 mg/Kg).

2.4 RNA sequencing and differential expression analysis

Total RNA was isolated from liver and testis (miRNeasy Mini kit, Qiagen) and sequenced as previously described for the liver samples (Dahl et al., 2021); testis libraries were prepared identically but sequenced as a separate batch (available at Annotare E-MTAB-17355). To allow

direct cross-tissue comparison, both tissues were processed through a single pipeline: reads were quantified with the nf-core/rnaseq pipeline v3.21.0 (Ewels et al., 2020) using Salmon against the GRCm39 mouse reference genome, summarised to gene level with the tximeta package (Love et al., 2020). Bioconductor packages in R were used downstream: Differential expression was modelled per tissue in DESeq2 (v1.52) with the design ~ strain + As_dose * IR, treating strain as a blocking factor. Genes with <100 summed counts and irrelevant mitochondrial/nuclear rRNA and tRNA genes were removed. Log2 fold changes were shrunk with apeglm 1.34 (single coefficients) or ashr 2.2-63 (composite contrasts). Genes with padj < 0.05 (Benjamini–Hochberg) and |log2FC| > 0.5 were considered differentially expressed.

2.5 Functional enrichment

Enrichment results were integrated with several Bioconductor packages: differential-expression statistics, visualisation and pipeline in GeneTonic 3.6 (Marini et al., 2021). Over-representation (ORA) of differentially expressed genes (DEG) and gene-set enrichment analysis (GSEA) of the full signed-ranked gene list were performed for GO Biological Process (GOBP) and Molecular Function (GOMF) with topGO 2.64, KEGG and Reactome pathways (clusterProfiler 4.20.0, ReactomePA 1.56), and the MSigDB Hallmark collection (msigdbr 26.1). GSEA used the DESeq2 Wald statistic as the ranking metric. GOBP redundancy was reduced by semantic similarity (rrvgo 1.24). ORA/GO terms were considered significant at padj < 0.05 and GSEA at padj < 0.25 (Benjamini–Hochberg). Several KEGG infection-disease gene sets were excluded as innate-immune/inflammatory proxies rather than relevant pathways.

Gene-set enrichment (GSEA) and over-representation (ORA) analyses (GO, KEGG, Reactome and MSigDB Hallmark) were summarised across all contrasts in both tissues. A pathway was scored as concordant when significant in liver and testis within the same contrast. ORA hits indicate perturbation without a direction, while the GSEA normalised enrichment score (NES) signifies whether the genes driving each enrichment in the genset is up- or down-regulated. The GSEA results are reported in detail. The heatmaps in Online Resource 3 are based on $-\log_{10}$ padj for the pathway, Table 2 presents mean $-\log_{10}$ padj for all pathways in the group.

2.6 miRNA profiling

Circulating miRNAs were the 21 previously profiled in this cohort (Duale et al., 2020). Those miRNAs were selected for radiation response, not arsenite response, in a screen of 567 candidate miRNAs. We looked up the validated mouse targets of any arsenite-responsive miRNAs in miRTarBase 9, TarBase 9 and TargetScan 8 with multiMiR 1.34. These target genes were intersected with the liver and testis arsenite DEGs and tested for over-representation (hypergeometric) and concordance with the mRNA GSEAs.

2.7 Statistical analysis of apical endpoints

Genotoxicity, organ-weight, tissue-metal and miRNA endpoints were analysed blindly with a fixed-effects factorial ANOVA (arsenite × irradiation × strain, with two-way interactions) reported with F values. Least-squares means with 95% confidence intervals are reported alongside differences from control (as percentage change or absolute least square mean difference (Δ) with Dunnett's test, * p<0.05, ** p<0.01, *** p<0.001). Bayesian model-averaged inclusion BF_{incl} (Garofalo et al., 2024) are added for interpreting hypothesis support on the common scale (BF_{incl} >10 strong and >3 moderate evidence for H_A, between 0.33 and 3

equivocal, <0.33 moderate and <0.1 strong evidence for H_0). We used JMP v17.0 (SAS Institute, USA), JASP 0.19.1 Mac (JASP Team 2026) and R v4.6.0 in RStudio v 2026.05.1+225. We used the LLM Claude Sonnet 4.8 as a coding assistant.

3 Results

3.1 Exposure confirmation and absence of overt toxicity (Online Resource 1)

Arsenite caused no overt systemic toxicity at either concentration. Liver analyses of arsenic species revealed large differences between High As, Low As and control groups with no outliers and no difference between γ-exposed or not, affirming that the dosages were relevant. Hepatic zinc showed a dose dependent reduction under arsenite ($\boldsymbol{\beta}$ = -0.007, F = 5.81**, 20% reduction at High As).

The relative testes weights were 42 % reduced by irradiation (Δ = -27*** BW%, $BF_{incl} = \infty$), but no effect of As-exposure was seen. Relative liver, kidney, heart, and spleen weights were unchanged by arsenite, with Bayes factors favouring the null for the arsenic term in each case ($BF_{incl} \leq 0.5$). Blood glucose was likewise unaffected, although all were higher than in the pilot study. Body weights were moderately higher in the arsenite groups (7% up at 3 mg/L, BF_{incl} = 3.9) and not indicating toxicity.

Body weights and organ weights for the control and irradiated groups were reported in Dahl et al. (2025) except for a moderate reduction in the corrected spleen weights[1] due to γ exposure (F = 10.3 BF_{incl} = 6.12). Values for the arsenite and combined-exposure groups are new to this report. The genotoxic and transcriptional responses described below thus occurred in the absence of frank organ toxicity or growth impairment. Raw data and factorial ANOVA results are in Online Resource 1.

3.2 Oxidative DNA lesions but no chromosomal damage (Fig 1, Online Resource 1)

Arsenite increased the FPG-sensitive lesions without increasing single strand breakage, indicating that its genotoxic action in this model was predominantly oxidative. The total effect of arsenite on SSB/ALS across γ exposure was reduced the by 7 and 23 % in a linear regression ($\boldsymbol{\beta}$ = -0.6**, upper panel, Fig 1, ANOVA: F = 4.8, BF_{incl} = 4.7 – moderate support) while at the same time the radiation effect was strong (F = 11.26**, BF_{incl} = 15). the regression lines were the same, regardless of irradiation or not (no AsxIR-interaction).

Less obvious from Fig 1, the ANOVA revealed a clear increase in oxidative DNA lesions: FPG-sensitive damage increased with As-exposure by 30 % and 27 % (Low As: Δ = 4.41*** %TI, $p < 0.01$, BF_{incl} = 18.9; High As: Δ = 3.94** %TI, BF_{incl} = 4.06). The corresponding net oxidative signal (FPG minus SSB/ALS), increased by 62 % and 70 % for Low and High As (Δ = 4.93** %TI and 5.54*** %TI), with strong evidential support (BF_{incl} = 22.0 and 24.2).

Arsenite showed no effect on micronucleus frequency. MNRET and MNNCE did not differ from the contrasting controls (Low and High As versus Control and Low As + IR and High As + IR

[1] The implausibly high spleen weights reported, but rejected, in Dahl et al. (2025) have been corrected after detecting a mix-up with heart data at one termination event. Heart data were not reported previously.

versus Gamma (IR), Fig 1) or in the ANOVA. In both cases, the Bayes factors favoured the null ($BF_{incl} \approx 0.32$ for the arsenic terms) providing moderate evidence for the absence of effect rather than a non-significant result, indicating arsenite as non-clastogenic.

RET was 29 % and 36 % reduced after Low and High As exposure (Δ = -0.51 % and -0.65 %) There was a strong support for a bone marrow toxic effect (BF_{incl} = 9 and 50, Low and High As). However, this lowered proportion of RETs did not bias the MN-results for the single or combined exposures, showing that the assay was not compromised by the bone marrow suppression.

Gamma irradiation produced the opposite genotoxicity pattern. Irradiation induced a strong increase in SSBs (F = 11.26**, BF_{incl} = 15), but not in the FPG comet signal, and induced very strong MNRET and MNNCE reactions at this low dose rate (F > 263, $BF_{incl} = \infty$**,** easy to spot in Fig 1**)**.

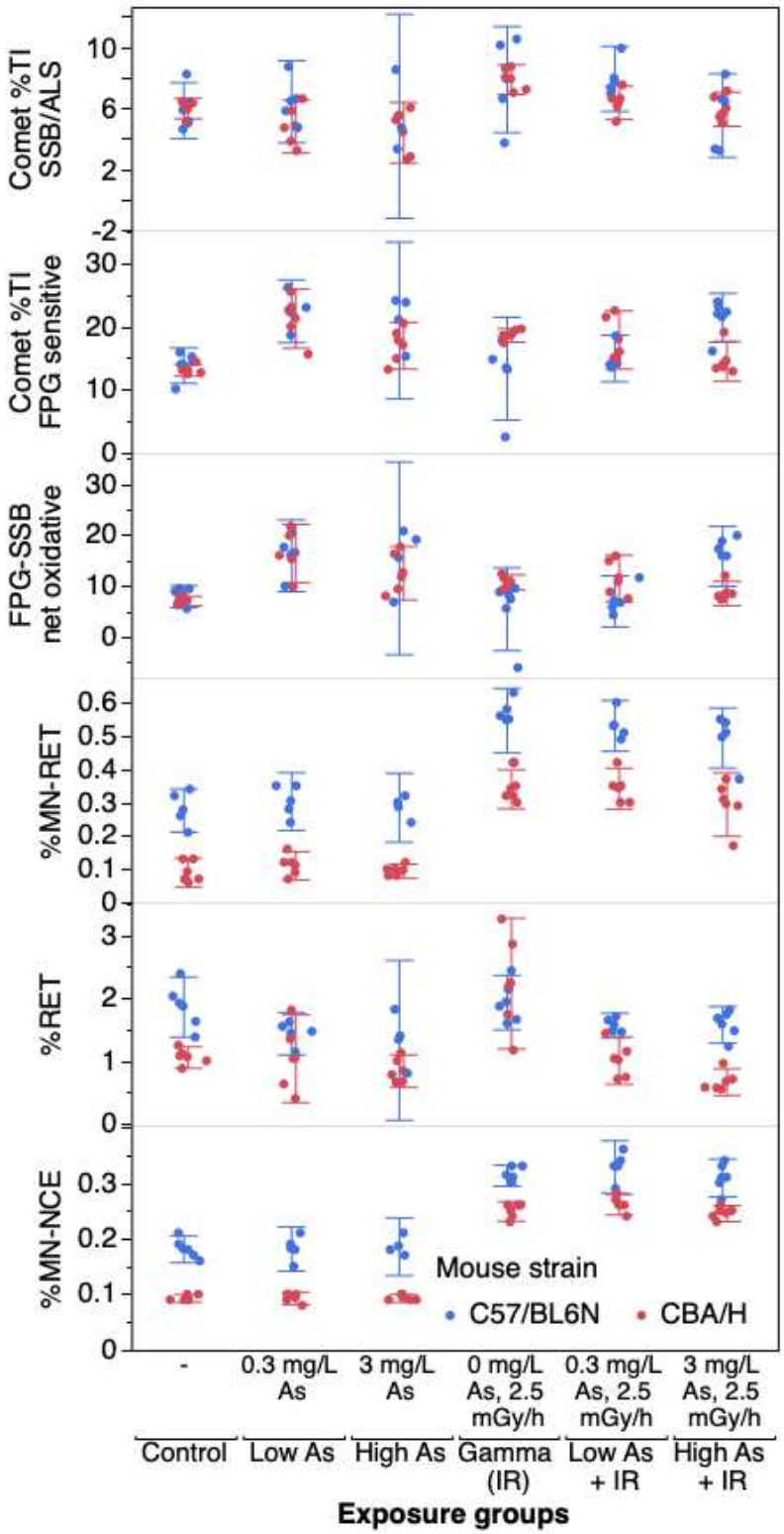


Fig 1 *DNA damage results: comet assay and micronucleus counts in blood cells. Error bars: 95% CI of mean providing a visual student's t-test.*

[PDF from JMP17]

3.3 Transcriptional: DNA-damage and oxidative-stress overview

In testis, radiation led to thousands of DEGs with hundreds of significant ORA/GSEA gene sets. The single-exposure groups produced substantially more DEGs relative to Control than the combined-exposure groups (Low As + IR, High As + IR) relative to Gamma (IR). In liver: 0 and 20 DEGs for the irradiated low- and high-arsenite groups versus 93-135 for low-high arsenite alone and 130 for irradiation. In testis: 10 and 17 DEGs for the irradiated low- and high-arsenite groups versus 229 and 124 for low-high arsenite alone and 3213 for irradiation.

Much of the single-exposure DEG response was lost under co-exposure. In testis there was a large irradiation response, as expected from the testis weight reduction.

GSEA, which is a threshold-free enrichment method, linked to many more pathways with direction of the response. The FPG-sensitive oxidative lesions related to arsenite exposure were accompanied by many significant DNA-repair pathways (Table 2). However, the categories differed quantitatively between organs. Oxidative phosphorylation was the most tissue-divergent category, strongly enriched in liver (mean $-\log_{10}$ padj: 7.9) but weaker in testis (mean $-\log_{10}$ padj: 2.78), with 8 pathways in each organ. Redox/glutathione was enriched chiefly under arsenite in liver but also under irradiation in testis. The xenobiotic/CYP450 metabolism was engaged strongly in testis, but stronger after irradiation than after As. The p53/apoptosis response was strongest under irradiation in testis.

The many similarities support the idea that the two organs share a DNA-damage and oxidative-stress response, while the differences illustrate that different downstream metabolic and stress programmes are recruited.

Table 2 Organ differences in DNA-damage-response and redox pathway categories (significant in both tissues within the same contrast). Mean $-\log_{10}$(padj), (number of pathways) in category.

	Arsenite (As)[1]		**Gamma (IR)[2]**		**AsxIR[3]**	
Pathway category[4]	Liver	Testis	Liver	Testis	Liver	Testis
DNA repair	1.4 (52)	1.4 (35)	2.13 (33)	2.16 (46)	2.4 (53)	1.8 (41)
Replication/cell cycle	1.34 (54)	1.38 (10)	3.05 (32)	1.87 (28)	2.91 (57)	1.8 (38)
p53/apoptosis	1.9 (20)	1.34 (15)	1.46 (4)	1.99 (20)	1.71 (11)	1.96 (22)
Oxidative phosphorylation	7.9 (8)	2.78 (8)	4.13 (5)	2 (2)	6.16 (8)	2.47 (4)
Redox/glutathione	2.74 (10)	0.95 (1)	1.46 (3)	2.42 (14)	2.76 (5)	1.58 (3)
Xenobiotic/CYP	1.61 (16)	2.65 (10)	1.22 (1)	3.91 (12)	1.52 (6)	1.2 (4)

[1.] Arsenite contrasts: Low As vs Control, High As vs Control, Low As and High As main effects
[2] Gamma contrast: Gamma (IR) vs Control
[3] AsxIR : interaction terms for Low As x IR and High As x IR
[4.] All pathways across significant ORA ($p < 0.05$)/GSEA ($p < 0.25$), pathway names in Online Resource 4

[5] Only GSEA reports normalised enrichment score (NAS). Directions differ from presented in Fig 2 where GSEA results are filtered according to $p<0.05$ and no ORAs are considered. Calculation is documented in Online Resource 4.

3.4 Arsenite and irradiation interaction, apical and transcriptional

The As-effect on SSB/ALS was down regardless of γ irradiation or not. This is a consistent antagonistic effect because of the *lack of* a statistical interaction. The As-effect on MNRET and MNNCE was null regardless of γ irradiation or not, because of the lack of a statistical interaction (BF_{incl} from 0.44 to 0.70)

In contrast, the FPG-sensitive lesion was not affected by γ irradiation (BF_{incl} = 1.9 - equivocal) while FPG increased after As-exposure. But the moderate but significant AsxIR interaction term (F = 11.62***, BF_{incl} = 7.38) appears because the strongest effect without γ was Low As, while High As was the stronger effect combined with γ (Fig 1, panel 2 from top). Thus, the As-induced total increase in FPG depended on Low As at single exposure, while on High As after gamma.

At the transcriptional level, the formal arsenite×irradiation interaction term (Table 2, As×IR column) was statistically well supported in both tissues, indicating that the combined response departed from the sum of the single-exposure responses. The same DNA-repair, oxidative-phosphorylation and redox programmes identified above indicate that concurrent arsenite modified the magnitude of the radiation response within these pathways rather than recruiting a distinct programme.

Filtering on the most significant pathways by $p<0.05$ for GSEA show a consistent downward regulation of the DNA-damage and oxidative-stress-cluster from both stressors (Fig 2). The exception was that the Oxidative phosphorylation, Redox/glutathione and the p53/apoptosis subsets were upregulated in testis. Low As seems to inflict the downward regulation more than High As, typically with larger gene sets. The interaction contrast between High and Low As is upregulation of Oxidative phosphorylation (liver and testis) and Carcinogenesis (liver only) indicating a shift in reaction pattern from Low to High As.

The combined exposures and interactions then flip the reaction pattern (Fig 2, right side of the red dashed vertical line): Almost all pathways were upregulated, with the exception of DNA Repair (KEGG) and DNA replication (Reactome, weak signal from KEGG) at the Low As + IR versus Gamma (IR) contrast. The stressor combination clearly changed the transcriptional landscape.



Fig 2 *Pathways associated with DNA repair and oxidative phosphorylation. GSEA analysis of KEGG, Reactome and Hallmark datasets, direction based on the normalised enrichment score.*

Contrasts: **Gamma (IR), Low As** and **High As** are the 3 single exposures contrasted to controls, **High vs Low As** contrasts arsenate only groups, **Low As | IR** and **High As | IR** contrast the combined exposures to Gamma (IR), **High vs Low As | IR** contrast the As + IR groups: **Low As x IR** and **High As x IR** are the interactions between each As-dose and IR overall. ▲ = GSEA pathway genes are on average shifted toward up-regulation (NES), ▼ = shifted down. The number of pathways presented is determined by automatic p-value selection without manual curation.

[pdf made in R added red lines and Contrasts: in Preview (Mac)]

3.5 Inflammatory and immune-related transcriptional responses (Fig 3)

Arsenite-associated inflammatory related pathways were strongly downregulated in the liver (Fig 3). Interferon response is similar to Fig 2, down in single exposures, up in combined and interactions. In contrast to Fig 2, single exposure High As here elicits a stronger signal than Low As, also confirmed by the interaction. The combined Low As | IR contrast shows that Low As adds further downregulation to irradiation alone, while High As | IR counters the irradiation signal in stark contrast to the Low As | IR signal (as shown by the Hi vs Lo As | IR and High As x IR interactions). A subjective impression is that the immune system is more resilient to both stressors than the DNA repair-oxphos system (no statistic test done).

In testis, the corresponding signal was qualitatively different where all pathways were upregulated except after single Low and High As exposure. The dominant non-repair response in testis was immune/inflammatory and radiation-driven: interferon-α and interferon-γ responses, TNFα/NF-κB and IL6–JAK–STAT3 signalling, and Toll-like/NOD-like receptor pathways were enriched under irradiation (mean $-\log_{10}$ padj for the innate-immune/interferon block ≈2.8 under irradiation versus ≈1.3 under arsenite). A parallel set of KEGG infection-disease gene sets not included here share large innate-immune gene memberships and are interpreted here as a generic inflammatory signature rather than as specific infections, showed the same irradiation-driven pattern in testis.



Fig 3 *Transcriptional response pathways associated with immune function. GSEA analysis of KEGG, Reactome and Hallmark datasets, direction based on the normalised enrichment score.* Extended legend in Fig 2, except that disease associated pathways are removed (eg., tuberculosis, malaria in KEGG)

3.6 miRNA response to arsenite

The radiation selected circulating-miRNA signature (Duale et al., 2020) was re-examined for arsenite effects using the factorial model. Only three miRNAs showed any arsenite effect. miR-133a-5p was the clearest, down-regulated by both arsenite and ionizing radiation (fold change vs control (FC) =0.65** BF_{incl}= 11.16 (Low As) and FC =0.63** BF_{incl}= 7.3 (High As); summarised to a strong arsenic main effect (BF_{incl}= 20). miR-26b-5p and miR-188-3p showed weaker associations to arsenite with equivocal Bayes factors. However, there were clear associations between miR-188-3p and radiation (F =8.74** BF_{incl}= 10) and strain (F =12.6** BF_{incl}= 38). miR-758-3p was also strongly associated with radiation (F =26.2** BF_{incl}= >100). The remaining 18 miRNAs were unaffected by arsenite (Online Resource 1). No consistent positive or negative correlation between miRNA and target direction was observed, and this could be expected from this small number of DEGs. We regard the miRNA findings as exploratory.

3.7 Additional pathway responses beyond DNA-damage (Online Resource 3)

In addition, the concordant enrichment fell into two broad themes metabolism and cardiovascular/contractile pathways each showing the same tissue partitioning seen for the core, with arsenite the dominant driver in liver and irradiation in testis. Metabolic enrichment in testis was comparatively weak, while the remaining liver pathways were dominated by primary hepatic functions like energy and intermediary metabolism (fatty-acid/lipid metabolism, adipogenesis and carbon/amino-acid metabolism). These radiation responses in hepatic metabolism are similar to previously reported for this liver model (Dahl et al., 2021). The new arsenite exposure predominantly up-regulated the amino-acid and protein-synthesis pathways (mean $-\log_{10}$ padj for carbohydrate/lipid metabolism: liver 2.7 versus testis 1.3).

Cardiovascular and contractile pathways (cardiac muscle contraction, vascular and fluid-shear-stress gene sets) followed the testicular, irradiation-driven, up-regulated pattern (testis 2.4 versus liver 0.9 for the irradiation effect. As these gene sets share large memberships with general muscle and cytoskeletal genes, they are interpreted as nonspecific contractile/structural signatures rather than cardiac-specific responses. A small set of non-oxidative cancer-pathway gene sets was likewise enriched only in irradiated testis.

3.8 Zink handling

The transcriptome showed a dose-related remodelling of zinc import: at the high dose the ZIP importers *Slc39a2*/ZIP2 (LFC 0.53) and *Slc39a5*/ZIP5 (−1.07) were differentially expressed, enriching the terms "zinc ion import across plasma membrane" and "zinc ion transmembrane transporter activity" (both padj = 0.014), whereas the gene expression of the zinc exporters (*Slc30a*/ZnT) and the metallothioneins was unchanged. Across animals, metallothionein expression (*Mt1*, *Mt2*) was correlated to the hepatic zinc levels (Spearman $\rho \approx 0.34$, padj ≈ 0.05) but was uncorrelated with the hepatic arsenic burden ($\rho \approx 0$, ns). This indicates that metallothionein followed zinc status through metal regulatory transcription factor 1 (MTF1) sensing rather than being induced by arsenite. Thus, the measured zinc loss was not buffered by sequestration. Other zinc-transport and zinc-finger repair genes showed no correlation with either metal after multiple-testing correction.

3.9 Strain effect is large but additive

The strains were mixed in all cages to avoid confounding effects between strain and cage. Still, we observed strain differences for many apical endpoints: MNRET, RET, MNNCE (Fig 1) body and organ weights, and for miR-188-3p. Strain×arsenite interaction was observed for FPG-comet and a strain×irradiation interaction for MNNCE.

Notably, the quality control measurements of arsenic species in the liver differed at High As (B6N higher, $p<0.01$) resulting in a strong strain×arsenite interaction (Online Resource 1).

There were also strain differences in the transcriptomics response. 4,270 genes in liver and 7,436 in testis were differentially expressed between CBA and B6N (Online Resource 2), an order of magnitude more than any treatment contrast. This large difference was additive with respect to the exposures. Strain×arsenite and strain×irradiation interaction terms identified few genes, significant for only 13 liver and 39 testis genes and equivalence testing confirmed that the irradiation response was statistically indistinguishable between strains for the great majority of genes (Online Resource 5).

In contrast to liver, the irradiation response in testis differed appreciably between strains: 815 genes showed a significant strain×irradiation interaction (versus 38 in liver), and irradiation elicited the largest transcriptional response of any effect in this tissue. A dose×strain asymmetry in the arsenite response was also evident: B6N responded predominantly to high arsenite whereas CBA responded predominantly to low arsenite (crossover $\chi2 = 2790$, $p < 10{-}300$ in testis; $\chi2 = 110$, $p = 1.2 \times 10{-}25$ in liver), with CBA showing a near-absent transcriptional response to high arsenite in testis. This pattern rests on lower-powered single-strain analyses.

4 Discussion

Three findings stand out: 1/ Arsenite was genotoxic through oxidative DNA damage rather than chromosomal breakage. 2/ The transcriptional responses to the two agents shared a common DNA-repair and oxidative-stress signature but diverged in the metabolic, immune and apoptotic programmes they recruited, in an organ-specific way. 3/ Concurrent exposure was non-additive, with arsenite mainly attenuating the radiation response.

4.1 Arsenite causes oxidative DNA damage and inhibits gene expression

Our findings do not support that arsenite is directly genotoxic. We could not challenge the current view that trivalent arsenic is a weak direct mutagen and a potent generator of reactive oxygen species and an inhibitor of DNA repair (Tam et al., 2020). A large number of reports have associated arsenite with direct strand breakage, but these studies are not comparable to our *in vitro* experiment regarding exposure levels and design. Our transcriptional data revealed mostly downregulated pathways after As exposure alone, including DNA repair pathways and a host of ROS-and cellular defence mechanisms.

We found that both arsenite and irradiation engaged a common set of highly significant DNA-repair, replication and cell-cycle-checkpoint pathways in liver and testis. However, downstream effects were stressor and organ specific. The downregulated liver responses were radiation driven cell cycle/DNA repair/oxidative phosphorylation and arsenite-driven redox, glutathione and xenobiotic metabolism, consistent with the liver's arsenic metabolism, methylation and biotransformation, processes that consume glutathione and generate reactive oxygen species.

While this response was expected after arsenate exposure, the similar results seen after γ irradiation was more interesting, representing a bona fide transcriptional footprint of genotoxic stress. There may be an energy-saving mechanism in the liver that lower the ROS defences after chronic low dose rate exposures. This state of adaptive suppression has been suggested after similar observations, but is still regarded as speculations (Feinendegen, 2016). The opposite could also be the case, that the stressor has crippled the liver's ability to respond to it.

The testis results may support a more plausible mechanism: the lowered DNA replication activity or cell-cycle arrest initiated to protect the germ cell populations, followed by a lowering of unnecessary DNA repair activity (Ding et al., 2017; Qin et al., 2008). At the same time the p53/apoptosis/oxidative phosphorylation/glutathione defence systems were upregulated to keep the guard up. This was opposite to the liver downregulation of both stressors and the testis downregulation after the reprotoxic arsenite (Zubair et al., 2017).

The RET reduction aligns with arsenic's established bone marrow toxicity that suppresses erythropoiesis through other mechanisms. Arsenate disrupts erythroid transcription factors and displaces Zn (Zhou et al., 2020), and we also observed an As-associated reduction of Zn in the liver.

4.2 Combined γ and arsenate may restore or enhance defence mechanisms

Our main co-exposure finding was that concurrent exposure to arsenite and irradiation was not additive. The combined-exposure groups in liver produced far fewer DEGs than either single exposure, indicating an attenuation of the single-agent response. In addition, many significant downregulated DNA-repair and oxidative-stress pathways engaged by the single exposures were pulling in the opposite direction. We interpret this as arsenite insults on top of irradiation are triggering the cellular responses into renewed efforts to maintain or improve the redox balance and DNA repair rather than adding an independent genotoxic insult. This non-additive, predominantly antagonistic interaction brings a new perspective on findings by others (Hornhardt et al., 2006; Mateuca et al., 2008; McDorman et al., 2002; Nuta et al., 2014).

4.3 An irradiation-driven interferon and inflammatory response

Our liver results showed anti-inflammatory effects after γ-irradiation or arsenite alone. Irradiation combined with Low As had an additive downregulating effect, while γ combined with High As antagonised this effect slightly. The exception was for the coagulation/complement group where all effects were additive anti-inflammatory.

The corresponding reactions in testis were all pro-inflammatory, clearly driven by the irradiation with an additive effect of both As-concentrations. This supports the idea that the testis' high radiosensitivity, with organ reduction and sterility, is mainly caused by inflammatory reactions and not genotoxicity. Arsenic alone had smaller, but anti-inflammatory, effect on the pathways.

Chronic low-dose-rate irradiation has shown immune hormesis and net anti-inflammatory effects with sustained cGAS–STING engagement driving interferon tachyphylaxis (Li et al., 2023). Arsenite has similarly been shown to suppresses JAK–STAT signalling at environmentally relevant doses (Xu et al., 2016) and chronic exposure could induce immunosuppression in the spleen with lowered interferon-associated transcripts (Yan et al., 2020). Each agent alone may therefore actively suppress the interferon response while their combination raises the genotoxic

and cytosolic-DNA burden sufficiently to cross some threshold level. This could explain the interferon response to combined arsenic and irradiation as threshold-dependent and providing both additive and non-additive inflammatory stimuli.

4.4 The effect of mouse strain

The arsenite and irradiation responses described above generalise across both genetic backgrounds, and strain is treated as an additive blocking factor rather than an effect modifier.

Differing mouse-strain susceptibility to ionizing radiation has been claimed repeatedly, but almost exclusively from microarray or phenotypic endpoints rather than RNA-seq (Jackson et al., 2017; Mukherjee et al., 2014; Ponnaiya et al., 1997; Snijders et al., 2012; Watson et al., 1997). We show consistent effects in both strains and tissues investigated. The strain effect was evident in the micronucleus assay, liver As-concentration and reticulocyte numbers, with interactions only for one endpoint (MNNCE).

We also found that the baseline expression of thousands of genes differed between CBA and B6. However, our strain×treatment test showed that the strain effect was additive with negligible interaction. It also showed that the liver irradiation response is strain-robust, whereas the testis response was clearly strain-dependent.

The GSEA analysis was performed on the entire transcriptome, ranked by the treatment-specific effect sizes derived from a two-way ANOVA. By explicitly accounting for and removing inter-strain variability in the model, we effectively minimized background noise. Thereby we increased the sensitivity to detect biologically coordinated, treatment-specific enrichment. The observed transcriptomic signals are therefore a robust rather than an artifact of DEG-list size. The multi-strain design has long been regarded as a way to increase the relevance for human extrapolation (Festing, 1995), and multi-organ evaluation is textbook toxicology.

4.5 Placing the findings in the adverse outcome pathway

The adverse outcome pathway AOP 296 links oxidative stress to genetic damage (Cho et al., 2022; Oxidative DNA Damage Leading to Chromosomal Aberrations and Mutations, 2023). Both arsenite and ionizing radiation generate reactive oxygen species; arsenite alone and via hepatic metabolites, radiation through water radiolysis. The first key event (KE), an increase in oxidative DNA damage (KE 1634), was measured directly as the FPG-sensitive comet increase with arsenite. The observed transcriptional engagement of base-excision repair (FPG) corresponds to a repair key event. The downstream adverse outcome of fixed chromosomal aberrations corresponds to our micronucleus findings. These three consecutive endpoints in one pathway may clearify the contrast between the two stressors: arsenite drove the network only as far as the oxidative-lesion and repair key events (comet-positive, micronucleus-negative), whereas irradiation drove it all the way to the micronucleus formation. Our doses of arsenite therefore behaved as initiators of the early, potentially reversible, key event without reaching the chromosomal-damage adverse outcome. This supports the recognised idea that arsenite is an oxidative co-mutagen rather than a direct clastogen.

5 Strengths and limitations

The main strength of this study is the factorial design applied to a single cohort, which lets the arsenite effect, the irradiation effect and their interaction be estimated jointly across genotoxic,

transcriptional and two-tissue readouts, with Bayesian evidence quantified alongside conventional testing. At the same time, the liver and testis samples were sequenced in two different batches in different laboratories, organ and analysis batch are confounded. The main limitations are a single late time point and only two arsenite concentrations; effect sizes were modest, as expected for environmentally relevant low-dose and low-dose-rate exposures. The enrichment analysis, while concordant across GO, KEGG, Reactome and Hallmark databases, rests partly on broadly annotated gene sets, and several KEGG infection-disease terms are interpreted as innate-immune proxies rather than literal pathways. Finally, the circulating miRNAs were measured in blood rather than in the sequenced tissues and was selected for radiation response, not arsenite.

6 Conclusion

Our data support H_A1: arsenite is genotoxic, but only through ROS/oxidising events at human relevant doses and not causing single strand breaks (supported by comet/micronucleus and transcriptomics). The hypothesis of an additive action (H_A2) should be supported for inflammatory reactions in the testis, but rejected for the other outcomes studied in testis and liver, where the interaction between stressors was non-additive, possibly antagonistic. H_A3 must be rejected: the stressor responses differed between the two strains, but with minimal strain×treatment interaction, justifying multi-strain studies.
Our study presents new data and improved experimental design and analysis methods for improving our understanding the genotoxic and transcriptional landscape of multiple stressor exposures.

Acknowledgements: from website

Conflict of interest: from website

7 References

Cho, E., Allemang, A., Audebert, M., Chauhan, V., Dertinger, S., Hendriks, G., Luijten, M., Marchetti, F., Minocherhomji, S., Pfuhler, S., Roberts, D. J., Trenz, K., & Yauk, C. L. (2022). AOP report: Development of an adverse outcome pathway for oxidative DNA damage leading to mutations and chromosomal aberrations. *Environmental and Molecular Mutagenesis*, *63*(3), 118–134. https://doi.org/10.1002/em.22479

Corcho Alvarado, J. A., Balsiger, B., Röllin, S., Jakob, A., & Burger, M. (2014). Radioactive and chemical contamination of the water resources in the former uranium mining and milling sites of Mailuu Suu (Kyrgyzstan). *Journal of Environmental Radioactivity*, *138*, 1–10. https://doi.org/10.1016/j.jenvrad.2014.07.018

Dahl, H., Olsen, A.-K., Berg, E., Duale, N., Hofer, T., Graupner, A., Brede, D. A., & Eide, D. M. (2025). Dose rate-driven responses to ionizing radiation in CBA/Ca and C57BL/6N evaluated using benchmark dose (BMD) modeling. *Science of The Total Environment*, *982*, 179589. https://doi.org/10.1016/j.scitotenv.2025.179589

Ding, X., Zhou, X., Cooper, K. L., Huestis, J., Hudson, L. G., & Liu, K. J. (2017). Differential sensitivities of cellular XPA and PARP-1 to arsenite inhibition and zinc rescue. *Toxicology and Applied Pharmacology*, *331*, 108–115. https://doi.org/10.1016/j.taap.2017.05.031

Duale, N., Eide, D. M., Amberger, M. L., Graupner, A., Brede, D. A., & Olsen, A. K. (2020). Using prediction models to identify miRNA-based markers of low dose rate chronic stress. *Science of The Total Environment*, *717*, 137068. https://doi.org/10.1016/j.scitotenv.2020.137068

Feinendegen, L. E. (2016). Quantification of Adaptive Protection Following Low-dose Irradiation. *Health Physics*. https://doi.org/10.1097/hp.0000000000000431

Festing, M. F. (1995). Use of a multistrain assay could improve the NTP carcinogenesis bioassay. *Environmental Health Perspectives*, *103*(1), 44–52. https://doi.org/10.1289/ehp.9510344

Garofalo, S., Finotti, G., Orsoni, M., Giovagnoli, S., & Benassi, M. (2024). Testing Bayesian Informative Hypotheses in Five Steps With JASP and R. *Advances in Methods and Practices in Psychological Science*, *7*(4), 25152459241260259. https://doi.org/10.1177/25152459241260259

Graupner, A., Eide, D. M., Instanes, C., Andersen, J. M., Brede, D. A., Dertinger, S. D., Lind, O. C., Brandt-Kjelsen, A., Bjerke, H., Salbu, B., Oughton, D., Brunborg, G., & Olsen, A. K.

(2016). Gamma radiation at a human relevant low dose rate is genotoxic in mice. *Scientific Reports*, *6*(1), 32977. https://doi.org/10.1038/srep32977

Graupner, A., Instanes, C., Andersen, J. M., Brandt-Kjelsen, A., Dertinger, S. D., Salbu, B., Brunborg, G., & Olsen, A.-K. (2015). Genotoxic effects of two-generational selenium deficiency in mouse somatic and testicular cells. *Mutagenesis*, *30*(2), 217–225. https://doi.org/10.1093/mutage/geu059

Hornhardt, S., Gomolka, M., Walsh, L., & Jung, T. (2006). Comparative investigations of sodium arsenite, arsenic trioxide and cadmium sulphate in combination with gamma-radiation on apoptosis, micronuclei induction and DNA damage in a human lymphoblastoid cell line. *Mutation Research - Fundamental and Molecular Mechanisms of Mutagenesis*, *600*(1–2), 165–176. https://doi.org/10.1016/j.mrfmmm.2006.04.002

IARC. (2012). *A review of human carcinogens*. International agency for research on cancer.

Jackson, I. L., Baye, F., Goswami, C. P., Katz, B. P., Zodda, A., Pavlovic, R., Gurung, G., Winans, D., & Vujaskovic, Z. (2017). Gene expression profiles among murine strains segregate with distinct differences in the progression of radiation-induced lung disease. *Dis Model Mech*, *10*(4), 425–437. https://doi.org/10.1242/dmm.028217

Li, J., Hubisz, M. J., Earlie, E. M., Duran, M. A., Hong, C., Varela, A. A., Lettera, E., Deyell, M., Tavora, B., Havel, J. J., Phyu, S. M., Amin, A. D., Budre, K., Kamiya, E., Cavallo, J.-A., Garris, C., Powell, S., Reis-Filho, J. S., Wen, H., … Bakhoum, S. F. (2023). Non-cell-autonomous cancer progression from chromosomal instability. *Nature*, *620*(7976), 1080–1088. https://doi.org/10.1038/s41586-023-06464-z

Love, M. I., Soneson, C., Hickey, P. F., Johnson, L. K., Pierce, N. T., Shepherd, L., Morgan, M., & Patro, R. (2020). Tximeta: Reference sequence checksums for provenance

identification in RNA-seq. *PLOS Computational Biology*, *16*(2), e1007664. https://doi.org/10.1371/journal.pcbi.1007664

Marini, F., Ludt, A., Linke, J., & Strauch, K. (2021). GeneTonic: An R/Bioconductor package for streamlining the interpretation of RNA-seq data. *BMC Bioinformatics*, *22*(1), 610. https://doi.org/10.1186/s12859-021-04461-5

Mateuca, R. A., Roelants, M., Iarmarcovai, G., Aka, P. V., Godderis, L., Tremp, A., Bonassi, S., Fenech, M., Bergé-Lefranc, J.-L., & Kirsch-Volders, M. (2008). hOGG1326, XRCC1399 and XRCC3241 polymorphisms influence micronucleus frequencies in human lymphocytes in vivo. *Mutagenesis*, *23*(1), 35–41. https://doi.org/10.1093/mutage/gem040

McDorman, E. W., Collins, B. W., & Allen, J. W. (2002). Dietary folate deficiency enhances induction of micronuclei by arsenic in mice. *Environmental and Molecular Mutagenesis*, *40*(1), 71–77. https://doi.org/10.1002/em.10085

Mukherjee, S., Sainis, K. B., & Deobagkar, D. D. (2014). F1 hybrids of BALB/c and C57BL/6 mouse strains respond differently to low-dose ionizing radiation exposure. *J Genet*, *93*(3), 667–682. https://doi.org/10.1007/s12041-014-0422-8

Nuta, O., Moquet, J., Bouffler, S., Lloyd, D., Sepai, O., & Rothkamm, K. (2014). Impact of long-term exposure to sodium arsenite on cytogenetic radiation damage. *Mutagenesis*, *29*(2), 123–129. https://doi.org/10.1093/mutage/get070

Oxidative DNA damage leading to chromosomal aberrations and mutations (OECD Series on Adverse Outcome Pathways No. 29; OECD Series on Adverse Outcome Pathways, Vol. 29). (2023). https://doi.org/10.1787/399d2c34-en

Ponnaiya, B., Cornforth, M. N., Ullrich, R. L., & New Collective Author. (1997). Radiation-induced chromosomal instability in BALB/c and C57BL/6 mice: The difference is as clear as black and white. *Radiation Research*, *147*(2), 121–125.

Qin, X.-J., Hudson, L. G., Liu, W., Ding, W., Cooper, K. L., & Liu, K. J. (2008). Dual actions involved in arsenite-induced oxidative DNA damage. *Chemical Research in Toxicology*, *21*(9), 1806–1813. https://doi.org/10.1021/tx8001548

Skipperud, L., Strømman, G., Yunusov, M., Stegnar, P., Uralbekov, B., Tilloboev, H., Zjazjev, G., Heier, L. S., Rosseland, B. O., & Salbu, B. (2013). Environmental impact assessment of radionuclide and metal contamination at the former U sites Taboshar and Digmai, Tajikistan. *Journal of Environmental Radioactivity*, *123*, 50–62. https://doi.org/10.1016/j.jenvrad.2012.05.007

Snijders, A. M., Marchetti, F., Bhatnagar, S., Duru, N., Han, J., Hu, Z., Mao, J.-H., Gray, J. W., & Wyrobek, A. J. (2012). Genetic differences in transcript responses to low-dose ionizing radiation identify tissue functions associated with breast cancer susceptibility. *PLoS One*, *7*(10), e45394. https://doi.org/10.1371/journal.pone.0045394

Tam, L. M., Price, N. E., & Wang, Y. (2020). Molecular Mechanisms of Arsenic-Induced Disruption of DNA Repair. *Chemical Research in Toxicology*, *33*(3), 709–726. https://doi.org/10.1021/acs.chemrestox.9b00464

Watson, G. E., Lorimore, S. A., Clutton, S. M., Kadhim, M. A., & Wright, E. G. (1997). Genetic factors influencing alpha-particle-induced chromosomal instability. *International Journal of Radiation Biology*, *71*(5), 497–503. https://doi.org/10.1080/095530097143824

WHO (with IPCS). (2001). *Arsenic and Arsenic Compounds* (2nd ed). World Health Organization.

Xu, H., Lauer, F. T., Liu, K. J., Hudson, L. G., & Burchiel, S. W. (2016). Environmentally relevant concentrations of arsenite and monomethylarsonous acid inhibit IL-7/STAT5 cytokine signaling pathways in mouse CD3+CD4-CD8- double negative thymus cells. *Toxicology Letters*, *247*, 62–68. https://doi.org/10.1016/j.toxlet.2016.02.014

Yan, N., Xu, G., Zhang, C., Liu, X., Li, X., Sun, L., Wang, D., Duan, X., & Li, B. (2020). Chronic arsenic exposure induces the time-dependent modulation of inflammation and immunosuppression in spleen. *Cell & Bioscience*, *10*(1), 91. https://doi.org/10.1186/s13578-020-00448-6

Zhang, X., Liu, Y., Xu, S., & Zhang, D. (2025). Arsenic compounds in cancer therapy: Mechanistic insights and antitumor activity. *Biochemical Pharmacology*, *240*, 117093. https://doi.org/10.1016/j.bcp.2025.117093

Zhou, X., Medina, S., Bolt, A. M., Zhang, H., Wan, G., Xu, H., Lauer, F. T., Wang, S. C., Burchiel, S. W., & Liu, K. J. (2020). Inhibition of red blood cell development by arsenic-induced disruption of GATA-1. *Scientific Reports*, *10*(1), 19055. https://doi.org/10.1038/s41598-020-76118-x

Zubair, M., Ahmad, M., & Qureshi, Z. I. (2017). Review on arsenic-induced toxicity in male reproductive system and its amelioration. *Andrologia*, *49*(9), e12791. https://doi.org/10.1111/and.12791

Supplementary Files

This is a list of supplementary files associated with this preprint. Click to download.

- OnlineResource5.docx
- OnlineResource1apical.xlsx
- OnlineResource4DDRredoxextract.xlsx
- OnlineResource3enrichmentsynthesis.xlsx
- OnlineResource2DEGenrichment.xlsx